

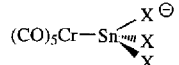
The present paper reports the synthesis and characterization of a series of stable compounds containing type **A** anions, **1**, and type **B** anions, **2**, including X-ray structures and ^{119}Sn -NMR data. The salt metathesis is described for the transformation of the stable $[\text{Ph}_4\text{P}]$ salts of type **B** anions into their reactive sodium salts. The substitution lability of the halides in these sodium salts is demonstrated by the preparation of an 8-oxoquinolato derivative, $[\{(\text{CO})_5\text{Cr}\}_2\text{Sn}(\text{oxinato})]$ (**4**), the structure of which is compared with that of $[\{(\text{CO})_5\text{Cr}\}_2\text{Sn}(\text{oxinato})_2]$ (**5**). The coordination behaviour of acetato-groups acting as X in type **B** anions, $[\{(\text{CO})_5\text{Cr}\}_2\text{EX}_2]^{2-}$, is analyzed for E = Sn, (**2g**), and E = Pb, (**3**), revealing a highly asymmetrical chelate binding mode for the carboxylato entities.

Results and Discussion

a) Compounds **1** Containing the $[\{(\text{CO})_5\text{M}\}\text{SnX}_3]^-$ Entity (M = Cr, Mo, W; X = Cl, Br, SiPr)

The disodium decacarbonyl dimetallates, $\text{Na}_2[\text{M}_2(\text{CO})_{10}]$ (M = Cr, Mo, W)^[5], react with SnX_2 (X = Cl, Br) in ethanol to yield a mixture of salts containing the well known stable anions of type **A**, $[\{(\text{CO})_5\text{M}\}\text{SnX}_3]^-$ ^[3], and of type **B**, $[\{(\text{CO})_5\text{M}\}_2\text{SnX}_2]^{2-}$ ^[4,6] (Scheme 1). The separation of these two classes of anions may be effected by the addition of salts such as $[\text{Ph}_4\text{P}]\text{Hal}$ and $[n\text{Bu}_4\text{N}]\text{Hal}$ which contain bulky cations. While the salts formed from these cations and type-**B** anions are almost insoluble in ethanol, the corresponding salts of type-**A** anions stay in solution. After the evaporation of the mother liquor the latter may be extracted selectively with diethyl ether. This type of procedure has been found to work for the whole series of compounds (M = Cr, Mo, W; X = Cl, Br); the procedure leading to **1a–c** have been developed in detail. It is essential that the precipitating agent contains the same halide constituent as does the coordinated $[\text{SnX}_3]$ entity of the organometallic species; partial exchange of the tin-bound halides with the halide introduced by the precipitating agent otherwise leads to a mixture of products.

Table 1. Complexes of type **A**

	no.	cation	X
	1a	$[\text{Ph}_4\text{P}]$	Cl
	1b	$[n\text{Bu}_4\text{N}]$	Br
	1c	$[\text{Ph}_4\text{P}]$	Br
	1d	$[\text{Na}-(12\text{-Crown-}4)_2]$	SiPr

The above procedure yields the compounds **1a–c** as yellow microcrystalline powders. Single crystals may be obtained by recrystallization from ethanol/diethyl ether. The formal analogue of **1a–c**, $[\{(\text{CO})_5\text{Cr}\}\text{Sn}(\text{SiPr})_3]^-$ (**1d**), has been obtained by the reaction of $\text{Na}_2[\{(\text{CO})_5\text{Cr}\}_2\text{SnCl}_2]$ ^[4] with sodium isopropylthiolate, $\text{Na}[\text{SiPr}]$, in THF. Even though compounds containing $[\{(\text{CO})_5\text{M}\}\text{SnX}_3]^-$ have been known for a long time^[3], the salts **1a–d** have not so far been fully characterized because X-ray structures and ^{119}Sn -NMR data are lacking for type-**A** anions.

In their IR spectra, compounds **1a–d** show a pattern of $\tilde{\nu}_{\text{CO}}$ absorptions which is characteristic of $[(\text{CO})_5\text{Cr}]$ units

(cf. Figure 2, Table 4)^[3]. Although three infrared-active bands ($2A_1 + E$) are expected for an idealized local C_{4v} symmetry^[7], it is apparent (cf. Figure 2) that only two of these three bands are observable. The A_1 band is believed to be accidentally degenerate with the E mode. The third weak shoulder observed in the IR spectrum of **1a** (1970 cm^{-1} ; Figure 2, Table 4) and **1d** (1950 cm^{-1} ; Table 4) is probably the IR-forbidden B_1 band which gains some intensity due to the distortion from pure C_{4v} symmetry^[3a,8].

The ^{119}Sn -NMR signals of **1** are consistently found in a range of $\delta = 344\text{--}170$ (Table 4) and clearly differentiate the mononuclear anions of type **A** contained in **1** from the dinuclear anions of type **B** contained in **2** (Table 4). The ^{119}Sn -NMR signal observed for **1a**, $\delta = 242$, is slightly shifted to lower field with respect to the known compound $[\{(\text{CO})_5\text{Cr}\}\text{SnCl}_2 \cdot \text{THF}]$ ($\delta = 192$)^[9] in which one of the tin bound chlorides is replaced by THF.

The structures of **1a**, **1b**, and **1d** have been determined by single crystal X-ray analyses (Figure 1, Tables 2 and 9). The basic arrangements are very much alike for all three anions and Figure 1 therefore shows only the structures of **1a** and **1d**. The compounds may be thought of as being composed of a $[\text{SnX}_3]^-$ donor ligand interacting with an acceptor $[(\text{CO})_5\text{Cr}]$ group. The isoelectronic relation between $[(\text{CO})_5\text{Cr}]\text{PX}_3$ ^[10] and $[\{(\text{CO})_5\text{Cr}\}\text{SnX}_3]^-$, seen even in spectroscopic data^[8], supports this view.

The tin atom is four-coordinate (Figure 1) with an overall geometry which is best described as distorted tetrahedral;

Figure 1. Molecular structures of the anions of **1a** and **1d**

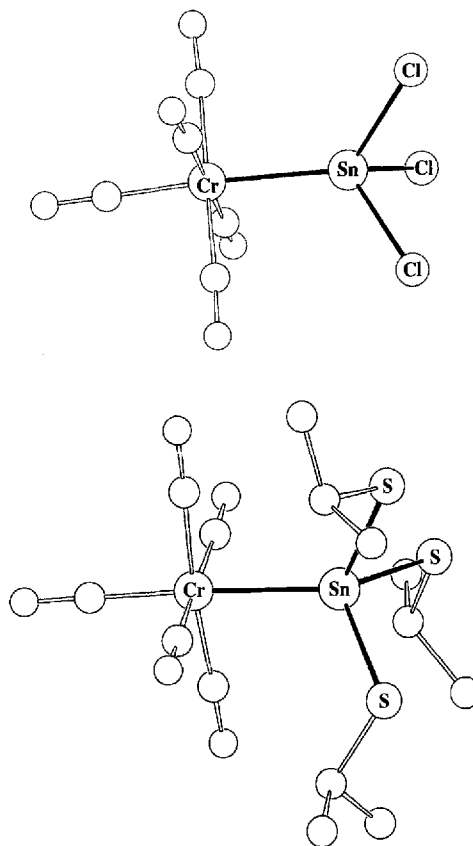


Table 2. Selected bond lengths [pm] and angles [°] of the anions of **1a**, **1b**, and **1d**^[a]

$[(\text{CO})_5\text{Cr}]\text{SnX}_3]^-$	1a ; X = Cl	1b ; X = Br	1d ; X = SiPr
Cr–Sn	258.3 (1)	256.0 (3)	262.7 (1)
Cr–C _{CO(ax)}	185.2 (3)	180 (2)	184.0 (9)
Cr–C _{CO(eq)} ^[b]	189.9 (4)	188 (2)	188 (1)
Sn–X	240.0 (1)	251.1 (3)	244.7 (3)
	239.0 (1)	252.6 (2)	251.0 (5)
	239.9 (1)	250.3 (3)	245.2 (3)
Cr–Sn–X	117.82 (3)	116.32 (9)	118.98 (8)
	125.34 (3)	124.55 (9)	115.6 (1)
	118.86 (3)	116.65 (9)	119.5 (1)
X–Sn–X	96.02 (4)	97.46 (9)	95.4 (1)
	96.19 (3)	98.06 (9)	92.0 (1)
	96.45 (4)	98.97 (9)	110.7 (1)
Sn–Cr–C _{CO(ax)}	174.8 (1)	174.8 (7)	176.7 (3)
Sn–Cr–C _{CO(eq)} ^[b]	90.0 (1)	92 (1)	87.9 (3)
C _{CO(eq)} –Cr–C _{CO(ax)} ^[b]	89.9 (1)	88 (1)	92.2 (4)
C _{CO(eq)} –Cr–C _{CO(eq)} ^[b]	90.0 (1)	90 (2)	89.9 (4)
Sn–S–C	–	–	101.6 (4)
	–	–	102.4 (4)
	–	–	103.7 (4)

^[a] Estimated standard deviations of the least significant figures are given in parentheses. – ^[b] Average values.

the mean Cr–Sn–X angles (X = SiPr: 118.0°, **1d**; X = Br: 119.2°, **1b**; X = Cl: 120.7°, **1a**) are larger than the average X–Sn–X angles (X = SiPr: 99.4°, **1d**; X = Br: 98.2°, **1b**; X = Cl: 96.2°, **1a**). The increase of the Cr–Sn–X angle and the accompanying decrease of the X–Sn–X angle, which go in parallel with the growing electronegativity of X, is also observed for a series of compounds which contain the isolobal $[\text{Cp}(\text{CO})_2\text{Fe}]$ moiety bound to the $[\text{SnX}_3]^-$ fragment^[11–13]. In these complexes the Fe–Sn–X angles increase in the series X = Ph (113.5°^[11]); X = Br (117.7°^[12]); to X = Cl (119.2°^[13]) while the X–Sn–X angles decrease (X = Ph: 105.3°^[11]; X = Br: 100.2°^[12]; X = Cl: 98.3°^[13]). The mean Sn–X distances observed for **1a**, **1b**, and **1d** (X = Cl: 239.6 pm; X = Br: 251.3 pm; X = SiPr: 247 pm) are distinctly shorter than those observed for the non-coordinated species $[\text{SnX}_3]^-$ ($[\text{Ph}_4\text{P}][\text{SnCl}_3]$: 247.0 pm; $[\text{Ph}_4\text{P}][\text{SnBr}_3]$: 262.4 pm; $[\text{Ph}_4\text{As}][\text{Sn}(\text{SPh})_3]$: 249.2 pm^[14]). This observation may be explained by the assumption that electron density is removed from the $[\text{SnX}_3]^-$ group by coordination to the $[(\text{CO})_5\text{Cr}]$ fragment, thereby increasing the π -contribution to the Sn–X bond^[15]. The mean Sn–X distances compare well with the average Sn–X bond lengths observed for the isoelectronic compounds $[(\text{Cp}(\text{CO})_2\text{Fe})\text{SnX}_3]$ (X = Cl: 235.8 pm^[13]; X = Br: 250 pm^[12]) and $[(\text{Cp}'(\text{CO})_2\text{Mn})\text{Sn}(\text{SMes})_3]$ (249.2 pm^[16], Mes = 2,4,6-trimethylphenyl). The Cr–Sn bond lengths (Cr–Sn: X = Cl, 258.3 pm, **1a**; X = Br, 256.0 pm, **1b**; X = SiPr, 262.7 pm, **1d**) lie well within the range of bond distances observed for other complexes containing a bond between a pentacarbonyl–chromium fragment and tin (256–262 pm^[17–19]).

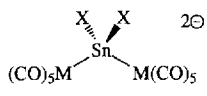
The idealized local C_{4v} symmetry of the $[(\text{CO})_5\text{Cr}]$ entity is slightly disturbed by the inherent C_{3v} symmetry of the $[\text{SnX}_3]^-$ group (Table 2). The Cr–C distance to the axial carbonyl group tends to be smaller than that to the equa-

torial CO ligands, since the $[\text{SnX}_3]^-$ ligands have a higher σ -donor to π -acceptor ratio as compared to the corresponding ratio of a CO group^[19].

b) Compounds **2** Containing the $[(\text{CO})_5\text{M}]_2\text{SnHal}_2]^{2-}$ Entity (M = Cr, Mo, W; Hal = Cl, Br)

The reaction of disodium decacarbonyl dimetallates, $\text{Na}_2[\text{M}_2(\text{CO})_{10}]$ (M = Cr, Mo, W)^[5], with tin(II) halides (Scheme 1) produces, in addition to the mononuclear anions of type **A**, **1a–c**, the dinuclear species $[(\text{CO})_5\text{M}]_2\text{SnHal}_2]^{2-}$ of type **B**, **2a–f**.

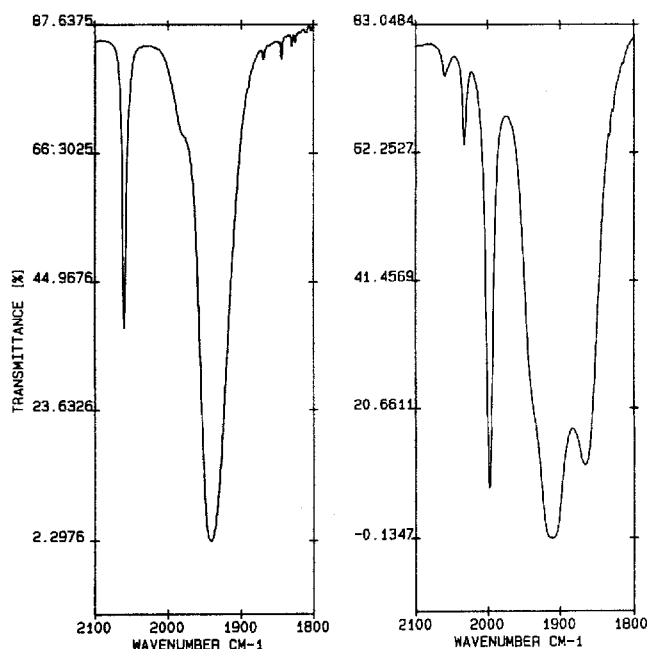
Table 3. Complexes of type **B**

	no.	cation	X	M
	2a	$[\text{Ph}_4\text{P}]$	Cl	Cr
	2b	$[\text{Ph}_4\text{P}]$	Cl	Mo
	2c	$[\text{Ph}_4\text{P}]$	Cl	W
	2d	$[\text{Ph}_4\text{P}]$	Br	W
	2e	$[\text{Ph}_4\text{P}]$	Br	Cr
	2f	$[\text{nBu}_4\text{N}]$	Br	Cr
	2g	$[\text{Ph}_4\text{P}]$	OOCCH ₃	Cr

Stable salts of these anions are precipitated from ethanol as yellow-orange powders upon addition of $[\text{Ph}_4\text{P}]\text{Hal}$ (vide supra). Crystals of these salts are obtained by recrystallization from THF/diethyl ether/petroleum ether 40/60 or dichloromethane/ethanol. As in the case of the isolation of compounds **1a–c**, it is essential to employ precipitating agents containing the same sort of halide as contained in the SnHal_2 part of the organometallic entity; a mixture of products generated by halide exchange is otherwise obtained.

The infrared spectra of the compounds **2a–f** show more than the three bands (cf. Figure 2, Table 4) expected on the basis of an idealized local C_{4v} symmetry of uncoupled $[(\text{CO})_5\text{M}]$ entities. The three strong $\tilde{\nu}_{\text{CO}}$ absorption bands are due to the infrared-active modes ($2A_1 + E$)^[7]. The distortion from pure C_{4v} symmetry (vide infra) results in the observation of an additional weak band, probably the IR-forbidden B_1 mode^[6,8]. Infrared spectroscopy is an efficient tool with which to analyze solutions for their relative content of type-A and type-B anions, due to the differences in the characteristic $\tilde{\nu}_{\text{CO}}$ patterns in the IR spectra of the compounds **1** and **2**.

Type-A and type-B anions are equally well discriminated against on the basis of their $^{119}\text{Sn}\{^1\text{H}\}$ -NMR data (Table 4). The resonances of the type-B anions are observed in a range of $\delta = 600$ –1000 (Table 4). The chemical shifts lie well within the range reported so far for organotin compounds^[20], as well as for transition metal tin complexes^[21] and are obviously not too much effected by the type of halide substituent X (X = Cl, Br). The resonances of the $[(\text{CO})_5\text{Cr}]$, **2a**, **2e**, and **2f**, and $[(\text{CO})_5\text{Mo}]$ compounds, **2b**, are all close to $\delta = 900$ –1000 (Table 4). The signals of the $[(\text{CO})_5\text{W}]$ compounds, **2c** and **2d**, consistently appear at around $\delta = 600$ (Table 4). The changes in the chemical shifts of heteronuclei are dominated by the paramagnetic contribution to the magnetic shielding^[22]. This paramagnetic term increases as the energy gap for the magnetic dipole allowed electronic excitation decreases. Following gen-

Figure 2. Carbonyl region of the infrared absorption spectra of **1a** and **2a** in THFTable 4. $\tilde{\nu}_{\text{CO}}$ -IR and $^{119}\text{Sn}\{^1\text{H}\}$ -NMR spectroscopic data for the compounds **1a–5**

		IR [a] ($\tilde{\nu}_{\text{CO}}$ / cm^{-1})			$^{119}\text{Sn}\{^1\text{H}\}$ [b] (δ / ppm)
1a	2055 (m)	1970 (sh)	1940 (vs)		242
1b	2055 (m)		1941 (vs)		171
1c	2054 (m)		1940 (vs)		170
1d	2032 (m)	1950 (sh)	1916 (vs)		344
2a	2029 (w)	1993 (s)	1910 (vs)	1862 (s)	924
2b	2040 (w)	2012 (s)	1919 (vs)	1865 (s)	912
2c	2041 (w)	2014 (s)	1914 (vs)	1862 (s)	604 [c]
2d	2041 (w)	2016 (s)	1915 (vs)	1862 (s)	623 [d]
2e	2027 (w)	1995 (m)	1913 (vs)	1869 (m)	994
2f	2028 (w)	1997 (s)	1915 (vs)	1869 (s)	1008
2g	2011 (m)	1993 (m)	1909 (vs)	1868 (m)	629
3	2050 (w)	2014 (s)	1929 (vs)		-
4	2037 (w)	2003 (s)	1922 (vs)	1918 (vs)	1176
5	2053 (m)		1934 (vs)		-47

[a] in THF, except **2g**, **3** in CH_2Cl_2 . – [b] in $[\text{d}_6]\text{acetone}$, 25°C . – [c] $^1J(^{183}\text{W}, ^{119}\text{Sn}) = 509 \text{ Hz}$; intensity ratio of peaks 15:100:15. – [d] $^1J(^{183}\text{W}, ^{119}\text{Sn}) = 506 \text{ Hz}$; intensity ratio of the peaks 14:100:13.

eral experience it may be assumed that this gap should be larger for $[(\text{CO})_5\text{W}]$ compounds when compared to $[(\text{CO})_5\text{Cr}]$ compounds; metal–ligand bonding is stronger in general for the tungsten derivatives than for the chromium complexes. Stronger bonding interactions imply, at the same time, stronger anti-bonding for unoccupied orbitals. The HOMO–LUMO gap will then be larger for tungsten containing compounds when compared to that of the analogous chromium complexes. The UV/Vis data (Table 7) do not contradict the assumptions made here. A larger HOMO–LUMO gap should, all other things staying equal, lead to a larger high-field shift in the NMR spectra. The high-field shift observed for the tungsten compounds, **2c**

and **2d**, relative to the chromium compounds, **2a**, **2b**, **2e**, and **2f**, is consistent with this model. The observed trend in chemical shifts compares well with analogous observations made for the series of compounds $[\{(\text{CO})_5\text{M}\}\text{SnCl}_2 \cdot \text{THF}]^{[9,23]}$. The same type of argument has been used to explain shift differences in ^{31}P -NMR spectroscopy^[24]. The observation of unconventional low-field shifts for the ^{119}Sn -NMR signals of the complexes, $[\{\text{Cp}^R(\text{CO})_2\text{Mn}\}_3(\mu_3\text{-Sn})]$ ($\text{Cp}^R = \text{Cp}$: $\delta = 3167$; $\text{Cp}^R = \text{Cp}'$: $\delta = 3185$; $\text{Cp}^R = \text{Cp}^*$: $\delta = 3301$) is also in support of the model discussed above; in these compounds a delocalized π -system^[25] leads to a small gap and consequently to a large paramagnetic contribution to the nuclear shielding.

For the pentacarbonyl–tungsten derivatives, **2c** and **2d**, the ^{183}W – ^{119}Sn coupling is clearly evident in the ^{119}Sn spectra; the intensity ratio of the ^{183}W satellites (natural abundance 14.3%^[26]) to the main signal is close to the value (ca. 28%) expected for, the statistical probability of the presence of ^{183}W for a species containing two equivalent tungsten nuclei coupling with one tin nucleus^[27,28]. The synthesis of **2c**, according to Scheme 1, is accompanied by the formation of $[\{(\text{CO})_5\text{W}\}\text{SnCl}_3]^-$, which has been characterized by IR spectroscopy^[3]. The presence of this species in the reaction mixture is also evident from the ^{119}Sn -NMR spectrum; $[\{(\text{CO})_5\text{W}\}\text{SnCl}_3]^-$ shows its signal at $\delta = -9$ ($[\text{D}_6]\text{acetone}$, 25°C). The intensity of the tungsten satellites [$^1J(^{183}\text{W}, ^{119}\text{Sn}) = 1360 \text{ Hz}$] is 14% of the intensity of the main ^{119}Sn -NMR signal, as expected for, the statistical probability of the presence of ^{183}W for a species containing a tin nucleus coupled to just one tungsten nucleus^[28]. The high-field shift of the ^{119}Sn -NMR resonance of this compound relative to the signals observed for its $[(\text{CO})_5\text{Cr}]$ analogous, **1a–d**, (Table 4) is thus in a similar range to that observed for the signals of the $[(\text{CO})_5\text{W}]$ derivatives, **2c** and **2d**, relative to their $[(\text{CO})_5\text{Cr}]$ analogous, **2a**, **2e**, and **2f**, (Table 4) and may be rationalized accordingly.

The X-ray structures of compounds, **2d** and **2f** (cf. Figure 3, Tables 5 and 10), are similar in general to the ones observed for their SnCl_2 analogues $[\{(\text{CO})_5\text{M}\}_2\text{SnCl}_2]^{2-}$ ($\text{M} = \text{Cr}, \text{Mo}, \text{W}$)^[4]. Thus the dianion, **2f**, is the bromine analogue of $[\{(\text{CO})_5\text{Cr}\}_2\text{SnCl}_2]^{2-}$, the structure of which has already been reported^[4], and **2d** is the bromine analogue of the previously structurally analyzed $[\{(\text{CO})_5\text{W}\}_2\text{SnCl}_2]^{2-}$ ^[4].

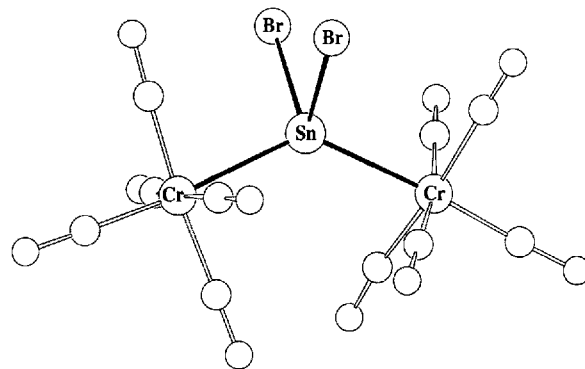
Figure 3. Molecular structure of the dianion of **2f**

Table 5. Selected bond lengths [pm] and angles [°] of the dianions of **2d**, **2f**, **2g**, and **3**^[a]

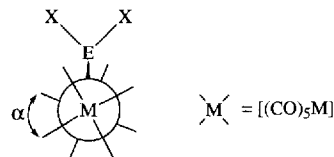
	2d , M = W, E = Sn, X = Br	2f , M = Cr, E = Sn, X = Br	2g , M = Cr, E = Sn, X = Oac	3 , M = Cr, E = Pb, X = Oac
M-E	280.9 (1) 280.9 (2)	264.0 (4) 264.4 (4)	268.4 (1) 268.4 (1)	272.2 (2) 272.6 (2)
M-CO(ax) [b]	197 (2)	182 (2)	183.9 (7)	184 (1)
M-CO(eq) [b]	203 (2)	188 (4)	187.6 (7)	189 (1)
E-X	258.9 (2) 261.3 (2)	260.4 (3) 260.8 (3)	218.8 (4) 218.8 (4)	235.8 (6) 235.3 (7)
E...O	-	-	288.5 288.5	289.2 286.7
M-E-M	130.62 (4)	131.6 (1)	130.72 (5)	147.85 (5)
X-E-X	92.24 (8)	92.3 (1)	80.3 (2)	74.3 (2)
M-E-X	109.44 (6) 102.06 (6) 107.15 (6) 108.49 (7)	103.9 (1) 105.5 (1) 106.9 (1) 109.5 (1)	107.2 (1) 109.9 (1) 107.2 (1) 109.9 (1)	103.3 (2) 102.7 (2) 102.7 (2) 102.4 (2)
M-E...O [b]	-	-	90.5	91.1
O-E...O [b]	-	-	48.7	48.8
O...E...O	-	-	128.6	123.0
E-Cr-CO(ax) [b]	174.8 (4)	175.0 (8)	173.7 (2)	177.5 (4)
E-Cr-CO(eq) [b]	87.1 (4)	86.3 (8)	86.5 (2)	87.7 (4)
CCO(eq)-Cr-CO(ax) [b]	92.9 (7)	94 (1)	93.6 (3)	92.2 (5)
CCO(eq)-Cr-CO(eq) [b]	89.8 (7)	89 (1)	89.9 (3)	89.9 (5)
	173.4 (6)	172 (1)	171.8 (3)	175.3 (5)

^[a] Estimated standard deviations of the least significant figures are given in parentheses. -- ^[b] Average values.

The molecular structure of **2** is depicted in Figure 3 with **2f** as the example.

Although the steric demands of bromine and chlorine substituents differ, the coordination of the tin centres is almost the same for the SnBr₂ derivatives, **2d** and **2f**, and their SnCl₂ analogues^[4]. The environment of the tin atom in **2d** and **2f** is distorted tetrahedral (Table 5). This overall geometry has been observed for the analogous compounds [((CO)₅M)₂SnCl₂]²⁻ (M = Cr, Mo, W)^[4], as well as for the isoelectronic complexes [Cp(CO)₃Cr]₂SnCl₂^[29], [((CO)₅-Mn)₂SnCl₂]^[30], [((CO)₅Mn)₂SnBr₂]^[30], [Cp(CO)₂Fe]₂-SnCl₂^[31], and [R₂(CO)₂Co]₂SnCl₂ (R = η⁴-2,3,5,6-norbornadiene)^[32]. It is especially noteworthy that the M-Sn-M angles stay closely around 128.5 ± 2.5° and the X-Sn-X angles closely around 95 ± 3° for the total sample of compounds (Table 5^[4,29-32]). These angles are obviously an intrinsic optimum for this type of compound and they are similar in their isoelectronic compounds [((CO)₅Cr)₂AsCl₂]⁻^[33,34] and [Cp'(CO)₂Mn]₂-SbCl₂⁻^[34]. The angles are clearly independent of the steric bulk and electronegativity of the substituents, as well as of the different lattice forces acting upon the anions in the different crystal environments. The Sn-W and Sn-Cr distances in the bromine compounds **2d** and **2f** (Table 5) are very similar to those reported for the chlorine derivatives (Sn-Cr: [((CO)₅Cr)₂SnCl₂]²⁻^[4] and [Cp(CO)₃Cr]₂-SnCl₂^[29]; Sn-W: [((CO)₅W)₂SnCl₂]²⁻^[4]). The agreement is equally good for all the other geometrical data, excluding, of course, the Sn-Br distances which are around 260 pm (Table 5), while the Sn-Cl distances average 248 pm^[4].

In the compounds **2a-f** each transition metal atom is in an approximately octahedral environment with a slight distortion from the idealized local C_{4v} symmetry; this is also obvious in the carbonyl region of the infrared spectra (vide supra). The observation that the torsion angles C_{CO(eq)}-M-M-C_{CO(eq)}, α (Figure 4), of the compounds [((CO)₅M)₂SnHal₂]²⁻ (M = Cr; X = Cl: 28°^[4], X = Br: 34°; M = W; X = Cl: 40°^[4]; X = Br: 38°) lie around 35°, indicates that a type of staggered orientation is the conformation preferred by the compounds.

Figure 4. Newman projection of a compound of type **B**; view along the M-M axis

c) Compounds Containing Anions of the Type

[((CO)₅Cr)₂E(OOCCH₃)₂]²⁻ (E = Sn, **2g**; E = Pb, **3**)

The modification of the given procedure by the introduction of lead as the main group centre into compounds of type **B** is hampered by the insolubility of PbCl₂, which only leads to anionic compounds of the general composition [((CO)₅M)Cl]⁻ (M = Cr, Mo, W)^[35]. With this experience a new synthetic strategy using the acetate instead of the halide salt has been developed, as Pb(OOCCH₃)₂ is somewhat more soluble.

Na₂[Cr₂(CO)₁₀] is first transformed into [Ph₄P]₂-[Cr₂(CO)₁₀] by salt metathesis with [Ph₄P]Cl in ethanol, a procedure similar to the one described for the preparation of [Et₄N]₂[Cr₂(CO)₁₀]^[5]. Addition of Pb(OOCCH₃)₂ to the orange solution of [Ph₄P]₂[Cr₂(CO)₁₀] in dichloromethane results in a colour change to deep red. [Ph₄P]₂[((CO)₅Cr)₂Pb(OOCCH₃)₂], **3**, is isolated in fair yields by evaporation of the solvent and thorough washing with THF and diethyl ether. Recrystallization from dichloromethane/diethyl ether yields the analytically pure, crystalline compound **3**. When, under otherwise equal reaction conditions, Sn(OOCCH₃)₂ is used instead of Pb(OOCCH₃)₂ the tin analogue of **3**, [Ph₄P]₂[((CO)₅Cr)₂Sn(OOCCH₃)₂] (**2g**) is obtained.

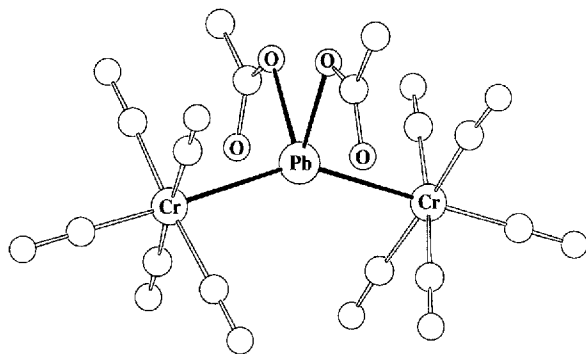
The $\tilde{\nu}_{\text{CO}}$ infrared spectrum of the bis(acetato)tin compound **2g** is in good accord with the type of spectrum observed for the compounds **2a-f** (Table 4), while the lead analogue **3** shows a new type of $\tilde{\nu}_{\text{CO}}$ infrared spectrum (Table 4), with only three $\tilde{\nu}_{\text{CO}}$ bands. The A₁ band is, as observed for **1a-d**, probably degenerate with the E mode (vide supra).

The signal in the ¹¹⁹Sn-NMR spectrum of **2g** (δ = 629) is strongly shifted to higher field (ca. 300 ppm) with respect to the values observed for the compounds [((CO)₅-Cr)₂SnHal₂]²⁻, **2a**, **2e**, and **2f**. This high-field shift may be explained by a higher coordination number (4 + 2) at the tin centre^[36] due to the ability of the acetate moieties to act as asymmetrical coordinating chelate ligands (vide infra).

For organotin compounds a similar shift has been found $[(n\text{Bu})_2\text{SnCl}_2]$: $\delta = 56$; $[(n\text{Bu})_2\text{Sn}(\text{OOCCH}_3)_2]$: $\delta = -195$ ^[20], thus supporting the above argument.

The X-ray structures determined for the compounds **2g** and **3** (cf. Figure 5, Tables 5, 10, and 11) are similar to the ones determined for organometallic dianions containing two pentacarbonyl–metal groups linked by an EHal_2 entity (vide supra).

Figure 5. Molecular structure of the dianion of **3**



Even for the acetato derivative **2g** the M–Sn–M angle (130.7° , Table 5) lies well within the range observed for the halide compounds (vide supra). The O–Sn–O angle (80° ; Table 5) is, however, substantially smaller than the Br–Sn–Br angles in **2d** and **2f** (92° ; Table 5) or the Cl–Sn–Cl angles observed in the chlorine analogues of **2d** (96° ^[4]) and of **2f** (94° ^[4]). This may reflect the fact that the acetato groups act as asymmetrically bonded chelate ligands, as is evident from Figure 5 for the lead analogue of **2g**. The corresponding mean distances for $\text{Sn}\cdots\text{O}$ (288.5 pm) and $\text{Pb}\cdots\text{O}$ (287.9 pm) (Table 5) are too small to neglect interactions between the oxygen atoms and the main group centre. The observed angles $\text{O}\cdots\text{Sn}\cdots\text{O}$ (177.3°) and $\text{O}\cdots\text{Pb}\cdots\text{O}$ (171.8°) are close to 180° (Figure 5, Table 5). A similar type of arrangement with weak interactions between the oxygen atom of an asymmetrically bonded chelate ligand and a tin centre is observed for the organotin acetato compound $[\text{R}_3\text{Sn}(\text{OOCCH}_3)]$ ^[37], the organotin nitrate species $[\text{Me}_2\text{Sn}(\text{NO}_3)_2]$ ^[38], and for the transition metal tin compound $[\{\text{Cp}(\text{CO})_2\text{Fe}\}_2\text{Sn}(\text{ONO})_2]$ ^[39]. While the overall geometries of **2g** and **3** closely correspond to each other, the difference in the Cr–E–Cr angles is noteworthy. The Cr–Sn–Cr angle observed for **2g** (130.7°) is in the range observed for the analogous $[\{(\text{CO})_5\text{Cr}\}_2\text{SnX}_2]^{2-}$ ($\text{X} = \text{Cl}, \text{Br}$) species (vide supra), while the Cr–Pb–Cr angle of 147.8° is substantially larger (Table 5). With reference to a corresponding increase in M–E–M angles in the series $[\{(\text{CO})_2\text{Cp}'\text{Mn}\}_2\text{EL}_2]$ ($\text{E} = \text{Ge}, \text{Sn}, \text{Pb}$; $\text{L}_2 = \text{bipyridine}, \text{phenanthroline}$)^[40,41], it may be inferred that the large Cr–Pb–Cr angle in **3** is not just a consequence of the specific substituent $(\text{OOCCH}_3)^-$, but reflects a general property of the compounds containing a lead-based ligand in the bridging position. Actually, the M–E–M angles reported for these chelate compounds are around 143.5° for the tin-centred species and around 148.2° for the lead-containing analogues^[40,41], indicating the same trend as for the

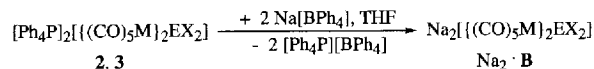
relevant angles reported here. Further weight is given to this argument by the observation that the same trend in M–E–M bond angles down a main group is also found for the isoelectronic series of compounds $[\{\text{Cp}'(\text{CO})_2\text{Mn}\}_2\text{E}(\text{bpy})]^+$ ($\text{E} = \text{As}, \text{Sb}, \text{Bi}$)^[34,42].

The idealized local symmetry of the $[(\text{CO})_5\text{Cr}]$ entity is slightly disturbed (Table 5), as might be expected from the IR spectra of **2g** and **3** (vide supra). In the case of **3**, the torsion angle, α (Figure 4), is observed to be 8.5° , while in **2g** the corresponding torsion angle is 22.8° .

d) Reactivity of the Compounds **2a–2g** and **3**

The salts **2a–g** and **3** are indefinitely stable at ambient temperature under inert conditions. They thus appear to be easy-to-handle starting compounds for further reactions. It is observed, however, that their reactivity is low^[43]. For instance, no reaction is observed when solutions of **2a** are treated with sodium 8-oxoquinolate, $\text{Na}[\text{C}_9\text{H}_6\text{NO}]$, while it is known that compounds of the type $[\{(\text{CO})_2\text{Cp}'\text{Mn}\}_2\text{Sn}(\text{oxinato})]^-$ are stable^[41]. In order to activate the anions of compounds **2** and **3** for reactions occurring in solution, an exchange of the bulky cations contained in these salts with solvated sodium ions proves helpful, as has already been seen from the preparation of **1d** (vide supra). This cation exchange is possible by salt metathesis of **2** and **3** with $\text{Na}[\text{BPh}_4]$ in THF.

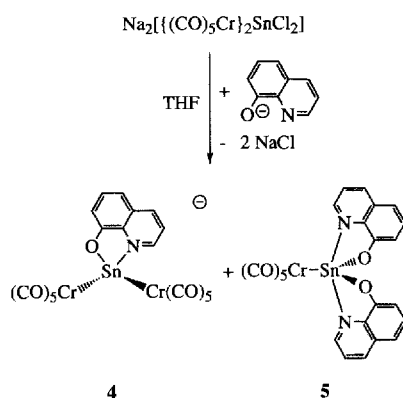
Scheme 2. Salt metathesis reaction



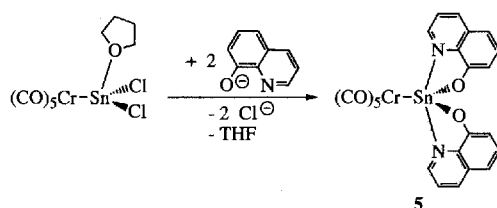
The salts $[\text{Ph}_4\text{P}][\text{BPh}_4]$ (**2a–e**, **2g**, **3**) or $[\text{nBu}_4\text{N}][\text{BPh}_4]$ (**2f**) precipitate immediately and yellow solutions containing the reactive sodium salts of type **B**, $\text{Na}_2[\{(\text{CO})_5\text{Cr}\}_2\text{EX}_2]$, are obtained. The identity of these salts is inferred, not only from the stoichiometry of the reactions where two equivalents of $[\text{Ph}_4\text{P}][\text{BPh}_4]$ or $[\text{nBu}_4\text{N}][\text{BPh}_4]$ are produced per equivalent of **2** or **3**, respectively, but is also corroborated by the infrared $\tilde{\nu}_{\text{CO}}$ -pattern of these sodium salts of type **B** compounds, which closely resembles the pattern observed for analogous salts containing the sodium cations in a 12-Crown-4 or [2,2,2]-Cryptand environment^[4]. Thus the THF solution of the sodium salt derived from **2a**, $[\text{Na}(\text{THF})_x]_2[\{(\text{CO})_5\text{Cr}\}_2\text{SnCl}_2]$ ($\tilde{\nu}_{\text{CO}}: \tilde{\nu} [\text{cm}^{-1}] = 2040 \text{ w}, 2007 \text{ s}, 2000 \text{ sh}, 1920 \text{ sh}, 1895 \text{ sh}$) shows $\tilde{\nu}_{\text{CO}}$ absorptions which are very similar to those observed with an authentic sample of $[\text{Na}-(12\text{-Crown-4})_2]_2[\{(\text{CO})_5\text{Cr}\}_2\text{SnCl}_2]$ in THF^[4]. The THF solutions of sodium salts derived from type **B** anions may be concentrated to yield THF solvates of the compounds as red oils, with the exception of the sodium salt obtained from **2b**, which decomposes upon concentration.

The increased reactivity of the sodium salts relative to the corresponding $[\text{Ph}_4\text{P}]$ salts is again demonstrated by repeating the reaction of sodium 8-oxoquinolate, $\text{Na}[\text{C}_9\text{H}_6\text{NO}]$ with the sodium salt derived from **2a**.

THF solutions of the sodium salt derived from **2a** react immediately with the oxinato ligand to produce solutions

Scheme 3. Reaction of $\text{Na}_2[\{(\text{CO})_5\text{Cr}\}_2\text{SnCl}_2]$ with sodium 8-oxoquinolate

which contain **4** as the main organometallic component. A small amount of **5** (vide infra) is formed as a by-product. The sodium salt of **4** may be separated by chromatography and crystallized after addition of 12-Crown-4 as $[\text{Na}-(12\text{-Crown-4})_2][\{(\text{CO})_5\text{Cr}\}_2\text{Sn}(\text{oxinato})]$; the by-product, **5**, may be crystallized as such. The low yields of **5** (10%) call for the development of a further, alternative, preparative route. It is found that $[\{(\text{CO})_5\text{Cr}\}_2\text{SnCl}_2 \cdot \text{THF}]^{[3b]}$ reacts with two equivalents of sodium 8-oxoquinolate in THF in a substitution reaction to produce **5** (Scheme 4) as the main product (70%). Compounds **4** and **5** are obtained in the form of yellow crystals.

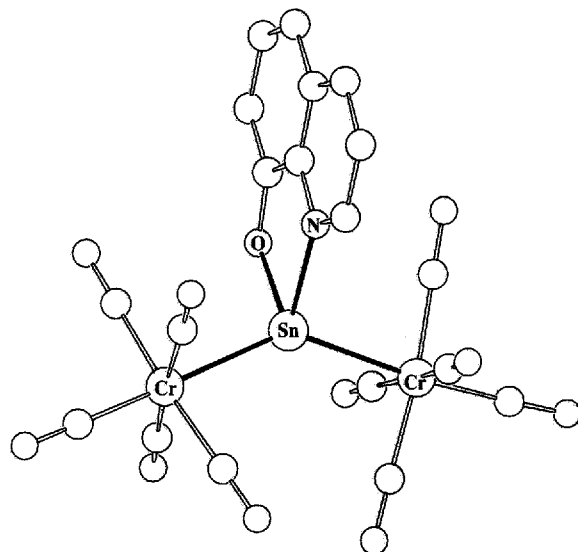
Scheme 4. Preparation of **5**

The $\tilde{\nu}_{\text{CO}}$ absorption pattern (Table 4) observed in the IR spectrum of **5**, containing a terminal tin-centred ligand, closely resembles the pattern characteristic for the compounds $[\{(\text{CO})_5\text{Cr}\}_2\text{SnX}_3]^-$, **1** (cf. Figure 2, Table 4), while the dinuclear compound, **4**, with its bridging tin-centred ligand, shows a $\tilde{\nu}_{\text{CO}}$ spectrum which is close to those observed for the dinuclear species, **2** (cf. Figure 2, Table 4).

The $^1\text{H-NMR}$ spectra reveal the presence of coordinated quinolato ligands (see Experimental Section). The $^{13}\text{C-NMR}$ signals of the quinolato ligand show that in both **4** and **5** only one type of chelate ligand is present, thus indicating the purity of **4** and the equivalence of the two quinolato ligands in **5** (Table 8). The $^{119}\text{Sn-NMR}$ signal of **4** is observed at $\delta = 1176$. It is somewhat low-field relative to the range observed for the dinuclear compounds **2** (Table 4). The $^{119}\text{Sn-NMR}$ signal of **5** is observed at $\delta = -47$. It is shifted to somewhat higher field with respect to the mononuclear compounds $[\{(\text{CO})_5\text{Cr}\}_2\text{SnX}_3]^-$, **1** (Table 4), which also contain a terminal tin-centred ligand, albeit with four-coordinate tin, in contrast to the five-coordinate tin

atoms in **5**. The same high-field shift due to the higher coordination number is observed for similar organotin compounds containing a chelating oxinato ligand ($[\text{Me}_3\text{SnCl}]$: $\delta = 164$; $[\text{Me}_3\text{Sn}(\text{oxinato})]$: $\delta = 48$)^[20].

The structure of the $[\text{Na}-(12\text{-Crown-4})_2]$ salt of **4**, $[\text{Na}-(12\text{-Crown-4})_2][\{(\text{CO})_5\text{Cr}\}_2\text{Sn}(\text{oxinato})]$, and of the THF solvate of **5**, have been determined by X-ray structural analyses (Figures 6 and 7, Tables 6 and 11).

Figure 6. Molecular structure of the anion of **4**Table 6. Selected bond lengths [pm] and angles [°] of the anion of **4** and **5**^[a]

	4 $[\{(\text{CO})_5\text{Cr}\}_2\text{Sn}(\text{ox})]^-$	5 · 1/2 THF $[\{(\text{CO})_5\text{Cr}\}_2\text{Sn}(\text{ox})_2]$
Cr-Sn	261.4 (1) 262.5 (1)	258.7 (2)
Cr-CCO(ax)	185.2 (5) [b]	183.5 (9)
Cr-CCO(eq) [b]	188.7 (5)	189.3 (8)
Sn-O	209.9 (3)	204.9 (4)
Sn-N	227.1 (4)	231.6 (5)
Cr-Sn-Cr	138.80 (3)	-
O-Sn-N	76.1 (1)	75.4 (2)
O-Sn-O	-	80.9 (2)
N-Sn-N	-	102.3 (2)
Cr-Sn-O	106.48 (8) 105.54 (8)	128.9 (1)
Cr-Sn-N	108.36 (8) 103.98 (8)	-
Sn-Cr-CCO(ax)	175.8 (2) [b]	180.0 [c]
Sn-Cr-CCO(eq) [b]	86.7 (2)	89.6 (2)
CCO(eq)-Cr-CCO(ax) [b]	93.3 (2)	90.4 (2)
CCO(eq)-Cr-CCO(eq) [b]	89.8 (2)	90.0 (4)
	173.2 (2)	178.8 (4)

[a] Estimated standard deviations of the least significant figures are given in parentheses. — [b] Average values. — [c] These atoms are located on a special position (twofold axis) of the space group (C2/c).

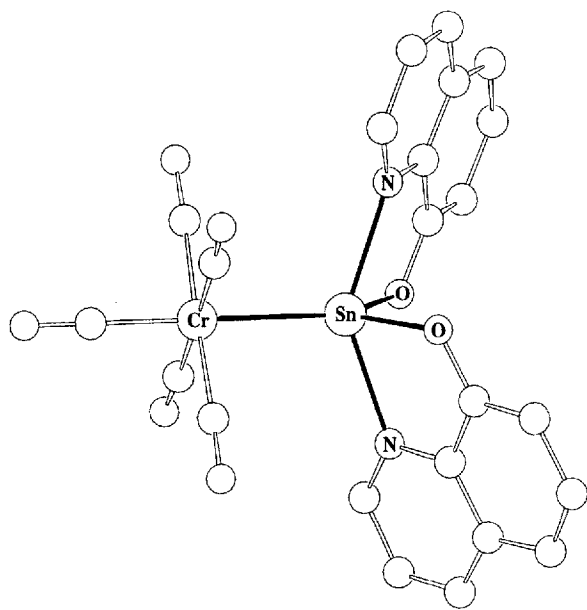
The coordination around the tin atom in **4** is distorted tetrahedral, corresponding to the arrangement observed for **2d** and **2f** (Figure 6, Tables 6 and 11), containing dicoordinated, bridging tin-centred ligands. the Cr-Sn-Cr angle in

4 (138.8°; Table 6) is somewhat larger than the equivalent angle in **2** (131°; Table 5). It closely corresponds to the Mn–Sn–Mn angle of 136.6° observed in the isoelectronic compound $[\{(\text{CO})_2\text{Cp}'\text{Mn}\}_2\text{Sn}(\text{oxinato})]^-$ ^[41]. The O–Sn–N angle (Table 6) is in good agreement with the analogous angles observed for $[\{(\text{CO})_2\text{Cp}'\text{Mn}\}_2\text{Sn}(\text{oxinato})]^-$ (73.9°)^[41] and the organotin compound $[\text{Me}_2\text{Sn}(\text{oxinato})_2]^-$ (73.6°)^[45]. The Sn–O and Sn–N distances in **4** (Table 6) are slightly shorter than in the related structures of $[\{(\text{CO})_2\text{Cp}'\text{Mn}\}_2\text{Sn}(\text{oxinato})]^-$ (Sn–O: 215.5, Sn–N: 231 pm)^[41] and $[\text{Me}_2\text{Sn}(\text{oxinato})_2]$ (Sn–O: 210, Sn–N: 235 pm)^[45].

The $\text{C}_{\text{CO}(\text{eq})}\text{--Cr--C}_{\text{CO}(\text{eq})}$ angles between the equatorial carbonyl groups are consistently smaller than the ideal angles of 90° and 180°, and correspond to Sn–Cr– $\text{C}_{\text{CO}(\text{eq})}$ angles of less than 90°, hence building the common umbrella-like structure^[46]. The mean torsion angle, α , (vide supra) in **4** is observed to be 28.9°.

5 is one of the rare structures showing a five coordinate tin centre^[47].

Figure 7. Molecular structure of **5**



As usual for five coordination, the overall geometry of **5** may be described in terms of a trigonal bipyramid, as well as in terms of a square pyramid. A trigonal bipyramidal arrangement may be imagined to have an equatorial CrSnO_2 plane, with the two nitrogen atoms occupying the apical positions (Figure 7). However, the N–Sn–N angle is 141.8° (Table 6), so the trigonal bipyramid is significantly distorted towards a square pyramid with chromium in the apical site. The mean O–Sn–N angles in the five membered chelate rings are 75.4° (Table 6) and the Sn–N bond lengthens by 5 pm in **5** compared to **4** (Table 6). The Cr–Sn distance (258.5 pm, Table 6) is somewhat shorter than the relevant distances observed for **2f**, **2g**, and **4**, and is, in effect, close to the distances observed for stannylene derivatives of $[(\text{CO})_5\text{Cr}]$ (e.g. $[\{(\text{CO})_5\text{Cr}\}\text{Sn}\{\text{CH}(\text{SiMe}_3)_2\}_2]$: 256.2 pm^[18]). It is substantially shorter than the distances re-

ported for base-stabilized stannylene complexes of the type $[\{(\text{CO})_5\text{Cr}\}\text{SnX}_2\text{L}]$ (e.g. $[\{(\text{CO})_5\text{Cr}\}\text{Sn}(t\text{Bu})_2\text{py}]$: 265.4 pm^[48]). It is not understood at present why even the twofold stabilization in **5**, with the two quinolato nitrogen atoms interacting with the tin centre (Figure 4, Table 6), still allows for the short Cr–Sn distance, as observed. A possible argument which explains this observation makes the assumption that the electronegative substituents in the dioxostannylene, present as a constituent in **5**, might compensate for the lengthening of the Cr–Sn bond which would be expected to result from the even twofold addition of donor functions to the stannylene moiety in **5**. The shortening of the mean Sn–O bond distance in **5** (204.9 pm), with respect to the corresponding distance in **4** (209.9 pm), gives further weight to this argument.

e) Concluding Remarks

Simple preparative strategies for the syntheses of a series of dinuclear complexes, $[\{(\text{CO})_5\text{M}\}_2\text{EX}_2]^{2-}$ have been made available. The $[\text{Ph}_4\text{P}]$ salts of these anions are easy to handle and are stable. It has been shown that the phosphonium cations in $[\text{Ph}_4\text{P}]_2[\{(\text{CO})_5\text{M}\}_2\text{EX}_2]$ may be exchanged by THF-solvated sodium cations. It has also been demonstrated that the reactivity of these sodium salts is greatly enhanced with respect to the relative inert nature of the analogous $[\text{Ph}_4\text{P}]$ salts. This increased reactivity has been shown by the syntheses of $[\text{Na}-(12\text{-Crown-4})_2][\{(\text{CO})_5\text{Cr}\}\text{Sn}(\text{SiPr})_3]$ (**1d**), and $[\text{Na}-(12\text{-Crown-4})_2][\{(\text{CO})_5\text{Cr}\}_2\text{Sn}(\text{oxinato})]$ (**4**), and awaits exploitation as a route for the preparation of compounds containing tin in a formal oxidation state below two.

Financial support by the *Deutsche Forschungsgemeinschaft* (SFB 247) and the *Fonds der Chemischen Industrie* is gratefully acknowledged.

Experimental Section

General: All manipulations were carried out under an argon atmosphere by means of standard Schlenk techniques at 20°C, unless mentioned otherwise. All solvents were dried by standard methods and distilled under argon. The photochemical reaction was carried out at 5°C in an isopropanol-cooled Duran-50 glass apparatus with a mercury lamp (TQ 150 Hanau). The $[\text{D}_6]\text{acetone}$ and CD_2Cl_2 used for the NMR spectroscopic measurements were degassed by three successive freeze-pump-thaw cycles and dried over 4 Å molecular sieves. The silica gel (Kieselgel z. A. 0.06–0.2 mm, J. T. Baker Chemicals B. V.) used for chromatography and the Kieselgur (Kieselgur, gereinigt, gegläht, Erg. B. 6, Riedel de Haen AG) used for filtration were degassed at 1 mbar at 180°C for 12 h and saturated with argon. – NMR: Bruker Avance DPX 200 at 200.13 MHz (^1H), 50.323 MHz ($^{13}\text{C}\{^1\text{H}\}$), 81.015 MHz ($^{31}\text{P}\{^1\text{H}\}$), 74.631 MHz ($^{119}\text{Sn}\{^1\text{H}\}$); chemical shifts (δ) in ppm with respect to $[\text{D}_6]\text{acetone}$ (^1H : δ = 2.04, ^{13}C : δ = 29.8) and CD_2Cl_2 (^1H : δ = 5.32, ^{13}C : δ = 53.5) as internal standards; chemical shifts (δ) in ppm with respect to 85% H_3PO_4 (^{31}P : δ = 0) and to SnMe_4 (^{119}Sn : δ = 0, at 25°C), respectively, as the external standard. – IR: Bruker FT-IR IFS-66; CaF_2 cells. – UV/Vis/NIR: Perkin Elmer Lambda 19; cells (0.2 cm; Hellma 110 suprasil). – MS (FAB): Finnigan MAT 8400; Nibeol (4-nitrobenzyl alcohol) or TEA (triethanol amine) matrices, respectively. – Elemental analyses: microanalytical

Table 7. Selected analytical data

	m.p. / °C	MS; <i>m/z</i> (%) [fragment]	UV / nm (THF) λ_{\max} (lg ϵ)	mol. formula (mol. mass)	elemental analysis
1a	117	417 (100) [(M - Ph ₄ P) ⁻]	295 (3.52, sh) 370 (2.84)	C ₂₉ H ₂₀ Cl ₃ CrO ₅ PSn (756.5)	calcd. C 46.04 H 2.66 found C 46.01 H 2.84
1b	75 - 78	551 (100) [(M - ⁿ Bu ₄ N) ⁻]	396 (2.90)	C ₂₁ H ₃₆ Br ₃ CrNO ₅ Sn (792.9)	calcd. C 31.80 H 4.58 N 1.77 found C 31.97 H 4.72 N 1.74
1c	118	551 (100) [(M - Ph ₄ P) ⁻]	389 (3.11)	C ₂₉ H ₂₀ Br ₃ CrO ₅ PSn (889.8)	calcd. C 39.14 H 2.27 found C 39.11 H 2.34
1d	191 (dec.)	537 (100) [(M - Na(12-C-4) ₂) ⁻]	293 (3.98, sh) 362 (3.08)	C ₃₀ H ₅₃ CrNaO ₁₃ S ₃ Sn (911.6)	calcd. C 39.53 H 5.86 found C 39.46 H 6.03
2a	208 - 212	536 (30) [(M - 2 Ph ₄ P - Cl) ⁻]	343 (4.05) 387 (3.89, sh)	C ₅₈ H ₄₀ Cl ₂ Cr ₂ O ₁₀ P ₂ Sn (1252.5)	calcd. C 55.62 H 3.22 found C 55.16 H 3.40
2b	155 (dec.)	577 (50) [(M - 2 Ph ₄ P - 3 CO) ⁻]	332 (3.64, sh) [a] 403 (3.66)	C ₅₈ H ₄₀ Cl ₂ Mo ₂ O ₁₀ P ₂ Sn (1340.4)	calcd. C 49.72 H 2.97 [b] found C 49.77 H 3.25
2c	179 (dec.)	781 (20) [(M - 2 Ph ₄ P - 2 CO) ⁻]	346 (3.57, sh) 417 (3.38)	C ₅₈ H ₄₀ Cl ₂ O ₁₀ P ₂ SnW ₂ (1516.2)	calcd. C 45.95 H 2.66 [c] found C 45.95 H 2.66 [c]
2d	191	870 (100) [(M - 2 Ph ₄ P - 2 CO) ⁻]	336 (4.04) 407 (4.00, sh)	C ₅₈ H ₄₀ Br ₂ O ₁₀ P ₂ SnW ₂ (1605.1)	calcd. C 43.40 H 2.51 found C 43.96 H 2.60
2e	181 (dec.)	606 (100) [(M - 2 Ph ₄ P - 2 CO) ⁻]	361 (4.03) 396 (3.93, sh)	C ₅₈ H ₄₀ Br ₂ Cr ₂ O ₁₀ P ₂ Sn (1341.4)	calcd. C 49.68 H 2.97 [d] found C 50.01 H 3.14
2f	175 (dec.)	606 (90) [(M - 2 ⁿ Bu ₄ N - 2 CO) ⁻]	433 (3.18)	C ₄₂ H ₇₂ Br ₂ Cr ₂ N ₂ O ₁₀ Sn (1147.5)	calcd. C 43.97 H 6.32 N 2.44 found C 42.67 H 6.65 N 2.46
2g	172 (dec.)	606 (25) [(M - 2 Ph ₄ P - CH ₃) ⁻]	319 (4.22) 363 (3.84, sh)	C ₆₂ H ₄₆ Cr ₂ O ₁₄ P ₂ Sn (1299.7)	calcd. C 55.93 H 3.53 [e] found C 56.25 H 3.72
3	172 (dec.)	650 (25) [(M - 2 Ph ₄ P - OOCCH ₃) ⁻]	318 (4.52) [a] 410 (3.57)	C ₆₂ H ₄₆ Cr ₂ O ₁₄ P ₂ Pb (1388.2)	calcd. C 52.47 H 3.31 [f] found C 52.98 H 4.12
4	178 (dec.)	648 (100) [(M - Na(12-C-4) ₂) ⁻]	310 (3.98) 432 (3.34)	C ₃₅ H ₃₈ Cr ₂ NNaO ₁₉ Sn (1022.3)	calcd. C 41.12 H 3.75 N 1.37 found C 41.10 H 3.96 N 1.41
5	213 (dec.)	600 (90) [M ⁻]	333 (3.72, sh) [a] 378 (3.93)	C ₂₃ H ₁₂ CrN ₂ O ₇ Sn (599.1)	calcd. C 42.15 H 2.06 N 4.10 [g] found C 42.28 H 2.11 N 4.01

[a] In dichloromethane. — [b] Calculated for **2b** · CH₂Cl₂. — [c] Not analytically pure. — [d] Calculated for **2e** · CH₂Cl₂. — [e] Calculated for **2g** · 0.5 CH₂Cl₂. — [f] Calculated for **3** · 0.5 CH₂Cl₂. — [g] Calculated for **5** · CH₂Cl₂.

laboratory of the Organisch-Chemisches Institut, Universität Heidelberg. — Melting points: Gallenkamp MFB-595 010; melting points have not been corrected. — DTG: TA 4000 System; Mettler; TC 11 TA-Processor; TG 50 Thermo scales (scales M3); argon; heating rate 10 K min⁻¹; Mettler Graphware TA 72. — The metalates of the composition Na₂[M₂(CO)₁₀] (M = Cr, Mo, W) were prepared as reported^[5]. All other chemicals were commercially obtained and used without further purification.

Salts 1 and 2 Containing the Trihalo(pentacarbonylchromium)stannate(II) Anions, [(CO)₅CrSnHal₃]⁻, and Dihalobis(pentacarbonylmetal)stannate(II) Dianions [(CO)₅M]₂SnHal₂]²⁻ (M = Cr, W)

a) [Ph₄P]₂[(CO)₅Cr]₂SnCl₂ (**2a**), [Ph₄P]₂[(CO)₅W]₂SnCl₂ (**2c**), [Ph₄P]₂[(CO)₅W]₂SnBr₂ (**2d**), [Ph₄P]₂[(CO)₅Cr]₂SnBr₂ (**2e**), [nBu₄N]₂[(CO)₅Cr]₂SnBr₂ (**2f**): To a stirred, orange solution of Na₂[M₂(CO)₁₀] (M = Cr, 430 mg; M = W, 694 mg; 1 mmol) in ethanol (50 ml) was added solid SnX₂ (X = Cl, 190 mg; X = Br, 278 mg; 1 mmol) in one portion. The solution turned deep red immediately. After stirring for 1 h the solution was filtered through Kieselgur (3 cm). By addition of [Ph₄P]Cl (**2a** and **2c**, 750 mg; 2 mmol), [Ph₄P]Br (**2d** and **2e**, 838 mg; 2 mmol) or [nBu₄N]Br (**2f**, 644 mg; 2 mmol) the corresponding orange salts precipitated immediately, except for **2f**, for which concentration of the solution (10 ml) proved necessary to induce precipitation of the salt. After stirring the solution for 1 h the solid was separated from the mother liquor by filtration and washed with cold ethanol (2 × 5 ml, 0 °C). The mother liquor was used for the isolation of the trihalostannate(II) salts. The isolation procedure was developed for **1a–c**: The orange precipitate was washed with diethyl ether (approximately 15 × 20 ml) to remove traces of

(pentacarbonyl-halo)metallates, [(CO)₅M}Hal]⁻ (M = Cr, W)^[35]. After the last washing step the ethereal solution should be colourless. Drying the salts in vacuo yielded the desired compounds as yellow-orange powders. The solid was dissolved in dichloromethane (20 ml) and filtered through Kieselgur (3 cm) to remove traces of unreacted precipitating reagent. Taking the solution to dryness left the compounds as yellow-orange microcrystalline solids, pure enough for further reactions. Yields: **2a**: 526 mg, 42%; **2c**: 576 mg, 38%; **2d**: 546 mg, 34%; **2e**: 469 mg, 35%; **2f**: 333 mg, 29%. To obtain analytically pure compounds the solids were again dissolved in dichloromethane (10 ml) and overlaid with ethanol (60 ml). Within two days the compounds precipitated as small orange crystals.

For growing single crystals of **2d** and **2f** the following procedure was carried out: A concentrated THF solution (5 ml) was shared out between three test-tubes (Ø = 1 cm), which were brought into a Schlenk tube (250 ml). Diethyl ether (30 ml), within the tube, was allowed to diffuse through the gas-phase into the THF-solution (3 h). After this period of time the diethyl ether was replaced by petroleum ether 40/60 (50 ml). Vapour diffusion of the petroleum ether 40/60 (7 days) yielded yellow single crystals suitable for X-ray structure analyses. **2a**: ¹H NMR ([D₆]acetone, 25 °C): δ = 7.89–7.83 (m, aromatic H). — ³¹P{¹H} NMR ([D₆]acetone, 25 °C): δ = 26.3 (s). **2c**: ¹H NMR ([D₆]acetone, 25 °C): δ = 7.89–7.83 (m, aromatic H). — ³¹P{¹H} NMR ([D₆]acetone, 25 °C): δ = 26.3 (s). — **2d**: ¹H NMR (CD₂Cl₂, 25 °C): δ = 7.89–7.83 (m, aromatic H). — ³¹P{¹H} NMR (CD₂Cl₂, 25 °C): δ = 26.4 (s). **2e**: ¹H NMR ([D₆]acetone, 25 °C): δ = 8.03–7.87 (m, aromatic H). — ³¹P{¹H} NMR ([D₆]acetone, 25 °C): δ = 24.2 (s). **2f**: ¹H-NMR ([D₆]acetone, 25 °C): δ = 3.43 (m, 16H, 1-H), 1.77 (m, 16H, 2-H), 1.39 (m, 16H, 3-H), 0.97 (t, 24H, 4-H).

Table 8. $^{13}\text{C}\{^1\text{H}\}$ -NMR data ($[\text{D}_6]\text{acetone}$, 25°C)

			acetato		S ⁱ Pr		[Ph ₄ P] ⁺ [a]				[ⁿ Bu ₄ N] ⁺ [b]				12-C-4
	CO _{ax}	CO _{eq}	C=O	CH ₃	CH	CH ₃	C-4	C-2	C-3	C-1	C-1	C-2	C-3	C-4	CH ₂
1a	226.1	218.3	-	-	-	-	136.4	135.7	131.4	119.0	-	-	-	-	-
1b	226.0	218.2	-	-	-	-	-	-	-	-	59.0	24.0	19.9	13.4	-
1c	226.4	218.6	-	-	-	-	136.4	135.7	131.4	119.0	-	-	-	-	-
1d	226.1	219.3	-	-	31.2	26.2	-	-	-	-	-	-	-	-	62.7
2a	232.9	225.5	-	-	-	-	136.4	135.5	131.5	118.7	-	-	-	-	-
2b	222.4	215.6	-	-	-	-	136.2	135.5	131.3	118.7	-	-	-	-	-
2c	211.4	206.6	-	-	-	-	136.5	135.5	131.5	118.7	-	-	-	-	-
2d	210.6	205.9	-	-	-	-	136.0	134.7	131.5	118.7	-	-	-	-	-
2e	232.4	225.2	-	-	-	-	136.0	135.2	131.0	118.5	-	-	-	-	-
2f	232.3	225.2	-	-	-	-	-	-	-	-	58.9	24.0	19.9	13.4	-
2g ^[c]	233.0	226.0	174.3	23.0	-	-	136.1	134.8	131.0	118.5	-	-	-	-	-
3 ^[c]	225.7	221.3	176.3	24.7	-	-	136.2	134.9	131.1	118.0	-	-	-	-	-
C-(oxinato)															
4	229.9	223.0	-	163.5	145.4	140.1	139.0	131.3	131.2	122.4	116.0	112.5	-	-	62.5
5	-	219.4	-	158.5	146.0	142.0	137.7	131.4	131.0	123.6	115.7	114.8	-	-	-

[a] C-1, C-2, C-3, and C-4 refers to C_{ipso} [d, $^1J(^{13}\text{C}, ^{31}\text{P}) = 89 \text{ Hz}$], C_{ortho} [d, $^2J(^{13}\text{C}, ^{31}\text{P}) = 10 \text{ Hz}$], C_{meta} [d, $^3J(^{13}\text{C}, ^{31}\text{P}) = 13 \text{ Hz}$], and C_{para} [d, $^4J(^{13}\text{C}, ^{31}\text{P}) = 3 \text{ Hz}$], respectively. – [b] C-1, C-2, C-3, and C-4 refers to C_{α} , C_{β} , C_{γ} , and C_{δ} , respectively. – [c] CD_2Cl_2 .

b) $[\text{Ph}_4\text{P}]_2[\{(\text{CO})_5\text{Mo}\}_2\text{SnCl}_2]$ (**2b**): To a stirred orange solution of $\text{Na}_2[\text{Mo}_2(\text{CO})_{10}]$ (518 mg; 1 mmol) in ethanol (50 ml), solid SnCl_2 (190 mg; 1 mmol) was added in one portion. The solution turned deep red immediately and was filtered through Kieselgur (3 cm) after stirring for 10 minutes. By addition of $[\text{Ph}_4\text{P}]\text{Cl}$ (750 mg; 2 mmol) a deep red salt precipitated spontaneously and was separated by filtration. The clear orange solution was taken to dryness and the resulting orange solid dissolved in THF to remove traces of unreacted $[\text{Ph}_4\text{P}]\text{Cl}$ by filtration. The resulting orange solution was taken to dryness, leaving an orange solid which was washed with diethyl ether ($20 \times 20 \text{ ml}$) and dried in vacuo. Yield: 201 mg, 15%. For further purification the orange solid was dissolved in dichloromethane (10 ml). This orange solution was poured dropwise into diethyl ether (100 ml) while **2b** precipitated immediately. After separation by filtration the yellow powder was dried in vacuo. **2b**: ^1H NMR ($[\text{D}_6]\text{acetone}$, 25°C): $\delta = 7.89\text{--}7.83$ (m, aromatic H). – $^{31}\text{P}\{^1\text{H}\}$ NMR ($[\text{D}_6]\text{acetone}$, 25°C): $\delta = 26.3$ (s).

c) Isolation of $[\text{Ph}_4\text{P}][\{(\text{CO})_5\text{Cr}\}_2\text{SnCl}_2]$ (**1a**), $[\text{nBu}_4\text{N}][\{(\text{CO})_5\text{Cr}\}_2\text{SnBr}_3]$ (**1b**), and $[\text{Ph}_4\text{P}][\{(\text{CO})_5\text{Cr}\}_2\text{SnBr}_3]$ (**1c**): After the separation of the yellow-orange salts of **2a**, **2e**, and **2f** from the reaction solution (vide supra) the remaining mother liquor was taken to dryness. The resulting red oil was extracted with diethyl ether ($25 \times 40 \text{ ml}$) until the extract was colourless. After removal of the solvent the remaining yellow precipitate was dried in vacuo. Yields: **1a** (197 mg, 26%); **1b** (190 mg, 24%); **1c** (213 mg, 24%). To obtain analytically pure compounds the yellow solids were dissolved in ethanol (10 ml), precipitated with diethyl ether (60 ml), separated by filtration, and dried in vacuo. Low temperature crystallization (-30°C) of **1a** and **1b** in ethanol/diethyl ether (1:1) yielded yellow crystals suitable for X-ray structure analyses within 14 days. **1a**: ^1H NMR ($[\text{D}_6]\text{acetone}$, 25°C): $\delta = 8.04\text{--}7.87$ (m, aromatic H). – $^{31}\text{P}\{^1\text{H}\}$ NMR ($[\text{D}_6]\text{acetone}$, 25°C): $\delta = 26.4$ (s). **1b**: ^1H NMR (CD_2Cl_2 , 25°C): $\delta = 3.15$ (m, 8H, 1-H), 1.59 (m, 8H, 2-H), 1.46 (m, 8H, 3-H), 1.02 (t, 12H, 4-H). – **1c**: ^1H NMR ($[\text{D}_6]\text{acetone}$, 25°C): $\delta = 8.09\text{--}7.87$ (m, aromatic H). – $^{31}\text{P}\{^1\text{H}\}$ NMR ($[\text{D}_6]\text{acetone}$, 25°C): $\delta = 24.3$ (s).

Bis(tetraphenylphosphonium) Bis(acetato)bis(pentacarbonylchromium)stannate(II) $[\text{Ph}_4\text{P}]_2[\{(\text{CO})_5\text{Cr}\}_2\text{Sn}(\text{OOCCH}_3)_2]$ (**2g**): To a stirred solution of $\text{Na}_2[\text{Cr}_2(\text{CO})_{10}]$ (430 mg; 1 mmol) in ethanol (50 ml), solid $[\text{Ph}_4\text{P}]\text{Cl}$ (750 mg; 2 mmol) was added in one portion. The orange $[\text{Ph}_4\text{P}]_2[\text{Cr}_2(\text{CO})_{10}]^{[5]}$ precipitated immediately

and was isolated by filtration. Washing the solid with ethanol ($2 \times 10 \text{ ml}$), THF ($2 \times 10 \text{ ml}$), and diethyl ether ($2 \times 10 \text{ ml}$) and drying in vacuo yielded the orange microcrystalline $[\text{Ph}_4\text{P}]_2[\text{Cr}_2(\text{CO})_{10}]$ salt in sufficient purity for further reactions. $[\text{Ph}_4\text{P}]_2[\text{Cr}_2(\text{CO})_{10}]$ (1063 mg; 1 mmol) was dissolved in dichloromethane (50 ml) and solid $\text{Sn}(\text{OOCCH}_3)_2$ (237 mg; 1 mmol) added in one portion. The resulting suspension gradually turned red and was stirred for 2 h. After filtration through Kieselgur (3 cm) the clear dark red solution was taken to dryness. The oily residue was washed with ethanol (20 ml), yielding a yellow powder which was separated by filtration and washed with ethanol ($2 \times 5 \text{ ml}$), THF ($2 \times 5 \text{ ml}$), and diethyl ether ($2 \times 5 \text{ ml}$) and dried in vacuo. Yield: 416 mg, 32%. For further purification the yellow powder was dissolved in dichloromethane (10 ml), overlaid with ethanol (60 ml) and stored in the dark. Within two days the compound precipitated in the form of small yellow crystals. **2g**: ^1H NMR (CD_2Cl_2 , 25°C): $\delta = 7.89\text{--}7.83$ (m, aromatic H), 1.88 (s, 6H, CH_3). – $^{31}\text{P}\{^1\text{H}\}$ NMR (CD_2Cl_2 , 25°C): $\delta = 23.5$ (s).

Bis(tetraphenylphosphonium) Bis(acetato)bis(pentacarbonylchromium)plumbate(II) $[\text{Ph}_4\text{P}]_2[\{(\text{CO})_5\text{Cr}\}_2\text{Pb}(\text{OOCCH}_3)_2]$ (**3**): To an orange solution of $[\text{Ph}_4\text{P}]_2[\text{Cr}_2(\text{CO})_{10}]$ (1063 mg; 1 mmol; vide supra) in dichloromethane (50 ml), solid $\text{Pb}(\text{OOCCH}_3)_2$ (325 mg; 1 mmol) was added in one portion. The resulting suspension gradually turned red and was stirred for 1 h. After filtration through Kieselgur (3 cm) the clear dark red solution was taken to dryness. The oily residue was washed twice with diethyl ether (20 ml) leaving an orange powder. This powder was washed with THF ($5 \times 20 \text{ ml}$) and diethyl ether ($2 \times 10 \text{ ml}$) and dried in vacuo. Yield: 278 mg, 20%. For further purification the orange powder was dissolved in dichloromethane (10 ml), overlaid with diethyl ether (60 ml) and stored in the dark. Within 5 days the compound precipitated in the form of orange crystals. **3**: ^1H NMR ($[\text{D}_6]\text{acetone}$, 25°C): $\delta = 7.93\text{--}7.87$ (m, aromatic H), 1.76 (s, 6H, CH_3). – $^{31}\text{P}\{^1\text{H}\}$ NMR ($[\text{D}_6]\text{acetone}$, 25°C): $\delta = 24.2$ (s).

Single Crystals of 2g and 3: A concentrated dichloromethane solution (5 ml) was shared out between three test-tubes ($\varnothing = 1 \text{ cm}$), which were brought into a Schlenk tube (250 ml). Diethyl ether (30 ml), contained within the tube, was allowed to diffuse through the gas-phase into the dichloromethane solution. Within 7 days in the dark, yellow (**2g**) and orange (**3**) single crystals suitable for X-ray structure analyses were obtained.

Cation Exchange in the $[Ph_4P]$ and $[nBu_4N]$ Salts **2 and **3**.** – **Preparation of the Sodium Salts:** The bulky organic cations were exchanged with the small sodium cation by treating solutions of **2** and **3**, respectively, with $Na[BPh_4]$. For this purpose 1 mmol of **2a–f** (**2a**: 1252 mg; **2b**: 1340 mg; **2c**: 1516 mg; **2d**: 1605 mg; **2e**: 1341 mg; **2f**: 1147 mg) was dissolved in THF (50 ml). In the case of **2g** and **3** (**2g**: 1300 mg; 1 mmol; **3**: 1388 mg; 1 mmol) dichloromethane (50 ml) was used as the solvent. To isolate the sodium salts, in each case $Na[BPh_4]$ (684 mg; 2 mmol) was added in one portion to the orange solution. $[Ph_4P][BPh_4]$ (**2a–e**, **2g**, **3**) immediately precipitated as a white solid. In the case of **2f**, the precipitate consisted of $[nBu_4N][BPh_4]$. The white $[BPh_4]$ salt was removed by filtration through Kieselgur (3 cm). The yellow solutions were evaporated in vacuo, except for the sodium salt derived from **2b** which decomposed upon concentration. The oily orange residues were dissolved in diethyl ether (20 ml). To remove remaining traces of $[BPh_4]$ salts the etheral solutions were again filtered through Kieselgur (3 cm). Evaporation of the solvent left the sodium-salts derived from **2a** (508 mg, 82%), **2c** (751 mg, 85%), **2d** (816 mg, 84%), **2e** (587 mg, 83%), **2f** (573 mg, 81%), **2g** (520 mg, 78%), and **3** (566 mg, 75%), respectively. The salts as derived from **2a–2g** and **3** were pure enough and immediately used for further transformations. The percentage yields as given relate to the idealized solvent free formula $Na_2[\{(CO)_5M\}_2EX_2]$.

Bis(12-Crown-4)sodium Tris(isopropylthiolato)(pentacarbonylchromium)stannate(II) $[Na(12-Crown-4)_2][\{(CO)_5Cr\}Sn(SiPr)_3]$ (**1d**): The sodium-salt derived from **2a** $Na_2[\{(CO)_5Cr\}_2SnCl_2]$ (310 mg; 0.5 mmol) was dissolved in THF (30 ml) and solid sodium isopropylthiolate, $Na[SiPr]$, (196 mg; 1 mmol) added in one portion. During stirring (1 h) a white precipitate ($NaCl$) formed which was removed by filtration through Kieselgur (3 cm). The clear yellow solution was concentrated to 5 ml and 12-Crown-4 (18 mg; 0.1 mmol) added. Single crystals of **1d** were obtained by applying the same procedure as for growing single crystals of **2d** and **2f**. Yield of yellow single crystals (after 14 days) was 173 mg (19%).

1d: 1H NMR (CD_2Cl_2 , 25°C): δ = 3.66 [s, 32H, CH_2 -(12-Crown-4)], 3.39 (sept, 3H, CH), 1.34 (d, 18H, CH_3).

Bis(12-Crown-4)sodium Bis(pentacarbonylchromium)(oxinato)stannate(II), $[Na(12-Crown-4)_2][\{(CO)_5Cr\}_2Sn(oxinato)]$ ($[Na(12-Crown-4)_2] \cdot 4$): 8-Hydroxyquinoline (72 mg; 0.5 mmol) was deprotonated with NaH (12 mg; 0.5 mmol) at $-70^\circ C$ in THF (30 ml). The solution was allowed to warm up slowly to $25^\circ C$ and was poured into a solution of the sodium salt derived from **2a**, $Na_2[\{(CO)_5Cr\}_2SnCl_2]$ (310 mg; 0.5 mmol) in THF (30 ml). The reaction mixture was stirred for 2 h, filtered through Kieselgur (3 cm) and taken to dryness. The oily orange residue was dissolved in diethyl ether (3 ml) and chromatographed on silica gel (10 cm; \varnothing = 3 cm). Elution with diethyl ether gave two bands. The first yellow band was identified by spectroscopic comparison (IR- and ^{119}Sn -NMR spectra) and found to be $[\{(CO)_5Cr\}Sn(oxinato)_2]$, **5**, which may be prepared more easily by a different procedure (vide infra). The second orange band contained unidentified products. An orange band which contained compound **4** eluted with THF. This THF fraction was concentrated to 5 ml and 12-Crown-4 (18 mg; 0.1 mmol) was added. Single crystals of **4** were obtained by applying the same procedure as for growing single crystals of **1d**, **2d**, and **2f**. Yield of yellow crystalline material (after 14 days) separated manually was 50 mg (10%). **4**: 1H NMR (D_6 acetone, $25^\circ C$): δ = 8.72 (m, 1H, oxinato-H), 8.43 (m, 1H, oxinato-H), 7.68 (m, 1H, oxinato-H), 7.48 (m, 1H, oxinato-H), 7.06 (m, 2H, oxinato-H), 3.65 [s, 32H, CH_2 -(12-Crown-4)].

(Pentacarbonylchromium)bis(oxinato)tin $[\{(CO)_5Cr\}Sn(oxinato)_2]$ (**5**): A stirred solution of $Cr(CO)_6$ (220 mg; 1 mmol) in THF (300 ml) was irradiated at $5^\circ C$ for 3 h. To the resulting yellow solution, $SnCl_2$ (190 mg; 1 mmol) was added in one portion. After stirring for 3 h at $50^\circ C$ the orange solution of $[\{(CO)_5Cr\}SnCl_2 \cdot THF]$ was concentrated to 100 ml. 8-Hydroxyquinoline (288 mg; 2 mmol) was deprotonated with NaH (48 mg; 2 mmol) at $-70^\circ C$ in THF (30 ml). The solution was allowed to warm up slowly to $25^\circ C$ and was poured into the orange solution of $[\{(CO)_5Cr\}SnCl_2 \cdot$

Table 9. Crystal structure data for **1a**, **1b**, and **1d**

compound	1a	1b	1d
formula	$C_{29}H_{20}Cl_3CrO_5PSn$	$C_{21}H_{36}Br_3CrNO_5Sn$	$C_{30}H_{53}CrNaO_{13}S_3Sn$
molecular mass [g]	756.460	792.920	911.60
crystal dimensions [mm]	0.30 x 0.30 x 0.30	0.30 x 0.40 x 0.25	0.30 x 0.30 x 0.30
crystal system	triclinic	triclinic	orthorhombic
space group (No.)	$P\bar{1}$ (2)	$P1$ (1)	$Pbca$ (61)
<i>a</i> [pm]	1078.8 (4)	1047.2 (6)	1579.0 (2)
<i>b</i> [pm]	1134.0 (3)	1158.6 (4)	2044.5 (6)
<i>c</i> [pm]	1395.3 (3)	1442.0 (1)	2588.6 (3)
α [°]	103.01 (2)	96.45 (5)	90.00 (0)
β [°]	109.20 (2)	92.26 (5)	90.00 (0)
γ [°]	95.58 (2)	114.24 (4)	90.00 (0)
cell volume [10^6 pm ³]	1543.2 (8)	1578 (2)	8356 (3)
molecular units / cell	2	2	8
density (calculated) [g cm ⁻³]	1.628	1.669	1.369
temperature [K]	200	295	200
no. rflns. for cell parameter refinement	35	25	25
scan range	$4.2^\circ \leq 2\theta \leq 52.0^\circ$	$3.9^\circ \leq 2\theta \leq 50.1^\circ$	$3.6^\circ \leq 2\theta \leq 56.0^\circ$
scan speed [° min ⁻¹]	$\dot{\omega} = 10$	$6.89 < \dot{\omega} < 29.3$	$\dot{\omega} = 13$
no. rflns. measured	6400	5589	10081
no. unique rflns.	6060	5589	10081
no. rflns. observed	5379	3114	4625
observation criterion	$I \geq 2\sigma$	$I \geq 2\sigma$	$I \geq 2\sigma$
no. parameters refined	362	321	518
residual electron density [$\cdot 10^{-6}$ e pm ⁻³]	0.71	1.06	1.10
R_I / R_w [%] (refinement on F^2)	2.9 / 7.3	8.8 / 24.1	9.1 / 28.0

Table 10. Crystal structure data for **2d**, **2f**, and **2g**

compound	2d	2f	2g
formula	C ₅₈ H ₄₀ Br ₂ O ₁₀ P ₂ SnW ₂	C ₄₂ H ₇₂ Br ₂ CrN ₂ O ₁₀ Sn	C ₆₂ H ₄₆ Cr ₂ O ₁₄ P ₂ Sn
molecular mass [g]	1605.090	1147.530	1299.620
crystal dimensions [mm]	0.30 x 0.20 x 0.30	0.40 x 0.40 x 0.10	0.20 x 0.30 x 0.30
crystal system	triclinic	orthorhombic	monoclinic
space group (No.)	P $\bar{1}$ (2)	Pna2 ₁ (33)	C2/c (15)
<i>a</i> [pm]	1171.6 (6)	3067 (2)	2371.8 (8)
<i>b</i> [pm]	1370.8 (7)	1542.2 (7)	1346.2 (5)
<i>c</i> [pm]	1869.3 (9)	1108.0 (6)	1963.5 (5)
α [°]	77.85 (2)	90.00 (0)	90.00 (0)
β [°]	78.93 (2)	90.00 (0)	111.47 (1)
γ [°]	82.61 (2)	90.00 (0)	90.00 (0)
cell volume [10 ⁶ pm ³]	2868 (3)	5241 (5)	5834 (3)
molecular units / cell	2	4	4
density (calculated) [g cm ⁻³]	1.853	1.454	1.473
temperature [K]	270	215	200
no. rflns. for cell parameter refinement	25	25	28
scan range	3.1° ≤ 2 θ ≤ 42.0°	3.0° ≤ 2 θ ≤ 48.2°	3.8° ≤ 2 θ ≤ 54.0°
scan speed [° min ⁻¹]	4.8 < $\dot{\omega}$ < 29.3	5.5 < $\dot{\omega}$ < 29.3	$\dot{\omega}$ = 12
no. rflns. measured	6414	4135	6529
no. unique rflns.	6145	4135	6377
no. rflns. observed	4578	2521	3955
observation criterion	<i>I</i> ≥ 2 σ	<i>I</i> ≥ 2 σ	<i>I</i> ≥ 2 σ
no. parameters refined	697	402	367
residual electron density [-10 ⁻⁶ e pm ⁻³]	0.61 · 10 ⁻⁶ e pm ⁻³	0.77	0.65
<i>R</i> / <i>R</i> _w [%] (refinement on F ²)	4.3 / 13.4	6.9 / 20.7	6.2 / 14.3

Table 11. Crystal structure data for **3**, **4**, and **5**

compound	3	4	5
formula	C ₆₂ H ₄₆ Cr ₂ O ₁₄ P ₂ Pb	C ₃₅ H ₃₈ Cr ₂ NNaO ₁₉ Sn	C ₂₃ H ₁₂ CrN ₂ O ₇ Sn
molecular mass [g]	1388.120	1022.350	599.034
crystal dimensions [mm]	0.20 x 0.30 x 0.20	0.20 x 0.30 x 0.30	0.30 x 0.20 x 0.30
crystal system	monoclinic	monoclinic	monoclinic
space group (No.)	P2 ₁ /c (14)	P2 ₁ /c (14)	C2/c (15)
<i>a</i> [pm]	2341.6 (2)	1433.6 (5)	1143.4 (5)
<i>b</i> [pm]	1310.7 (3)	1065.8 (3)	1819.8 (7)
<i>c</i> [pm]	2060.4 (3)	2819.1 (9)	1284.8 (4)
α [°]	90.00 (0)	90.00 (0)	90.00 (0)
β [°]	112.12 (1)	85.32 (3)	100.69 (3)
γ [°]	90.00 (0)	90.00 (0)	90.00 (0)
cell volume [10 ⁶ pm ³]	5858 (2)	4293 (2)	2627 (2)
molecular units / cell	4	4	4
density (calculated) [g cm ⁻³]	1.574	1.532	1.596
temperature [K]	200	200	230
no. rflns. for cell parameter refinement	30	25	25
scan range	3.8° ≤ 2 θ ≤ 47.0°	2.9° ≤ 2 θ ≤ 60.0°	4.3° ≤ 2 θ ≤ 46.0°
scan speed [° min ⁻¹]	$\dot{\omega}$ = 12	8.0 < $\dot{\omega}$ < 60.0	2.3 < $\dot{\omega}$ < 29.3
no. rflns. measured	6829	9004	2033
no. unique rflns.	6590	8701	1830
no. rflns. observed	4523	7243	1725
observation criterion	<i>I</i> ≥ 2 σ	<i>I</i> ≥ 2 σ	<i>I</i> ≥ 2 σ
no. parameters refined	613	539	177
residual electron density [-10 ⁻⁶ e pm ⁻³]	0.97	0.93	0.76
<i>R</i> / <i>R</i> _w [%] (refinement on F ²)	4.9 / 11.0	4.3 / 13.9	3.1 / 13.2

THF]. To remove traces of insoluble material after stirring for 3 h, the solution was filtered through Kieselgur (3 cm). The orange solution was taken to dryness, leaving 419 mg (70%) of crude **5** as a yellow powder. For further purification, **5** was dissolved in dichloromethane (10 ml) and overlaid with diethyl ether (100 ml). Within 2 days, **5** precipitated in the form of a yellow microcrystalline powder. Yellow single crystals of **5**, suitable for X-ray struc-

ture analyses were obtained after 14 days by applying the same procedure as for growing single crystals of **1d**, **2d**, **2f**, and **4**.

5: ¹H NMR ([D₆]acetone): δ = 9.15 (d, 1H, oxinato-H), 8.78 (d, 1H, oxinato-H), 8.04 (m, 1H, oxinato-H), 7.61 (m, 1H, oxinato-H), 7.40 (d, 1H, oxinato-H), 7.07 (d, 1H, oxinato-H).

X-ray Structure Determinations: The measurements for **1a**, **1d**, **2d**, **2e**, **2g**, **3**, and **4** were carried out on a Siemens P4 Dif-

fractometer. The data for **1b** were collected on a Siemens/(Stoe) AED2 apparatus. Both are four circle diffractometers with graphite-monochromated Mo- K_α radiation. The intensities of three test reflections (measured every 100 reflections) remained constant throughout the data collection, thus indicating crystal and electronic stability. All calculations were performed using the SHELXT PLUS software package. Structures were solved by direct methods with the SHELXS-86 program and refined with the SHELX93 program^[49]. Absorption corrections (ψ scan, $\Delta\psi = 10^\circ$) were applied to the data. The structures were refined in fully or partially anisotropic models by a full-matrix least-squares calculation. Hydrogen atoms were introduced at calculated positions. The data for the structure determination are compiled in Tables 9–11. Peculiarities of the structures are as follows: **1b**: The axial carbonyl group has been refined in a split position with three locations (occupation 0.4, 0.3, and 0.3) close to each other. Reasonable temperature factors have thus been obtained. **1d**: There is some disorder in the orientation of the SiPr groups which have been appropriately refined. The major rotamer is shown in Figure 1. **2d**: One of the phenyl rings of the two $[\text{Ph}_4\text{P}]^+$ counterions shows rotational disorder. This phenyl ring was refined isotropically. **2g**: The hydrogen atoms of the methyl group of the acetato ligands were not included in the refinement. **3**: Technical problems did not allow for experimental absorption correction; instead a numerical correction (DIFABS^[50]) was applied. **4**: One of the Crownether molecules shows disorder. **5**: The crystal analyzed contained 0.5 THF per molecule **5**. Further details of the crystal structure investigations may be obtained from the Fachinformationszentrum Karlsruhe, D-76344 Eggenstein-Leopoldshafen (Germany), on quoting the depository numbers CSD-406227 (**1a**), CSD-406224 (**1b**), CSD-406220 (**1d**), CSD-406221 (**2d**), CSD-406222 (**2f**), CSD-406225 (**2g**), CSD-406223 (**3**), CSD-406219 (**4**), CSD-406226 (**5**).

* Dedicated to Professor G. E. Herberich on the occasion of his 60th birthday.

- [1] B. Schiemenz, F. Ettel, G. Huttner, *J. Organomet. Chem.* **1993**, 456, 159–166.
- [2] B. Schiemenz, G. Huttner, *Angew. Chem.* **1993**, 105, 295–296; *Angew. Chem. Int. Ed. Engl.* **1993**, 32, 297–298.
- [3] [3a] J. K. Ruff, *Inorg. Chem.* **1967**, 6, 1502–1504. – [3b] D. Uhlig, H. Behrens, E. Lindner, *Z. Anorg. Allg. Chem.* **1973**, 401, 233–242. – [3c] T. Kruck, H. Breuer, *Chem. Ber.* **1974**, 107, 263–269. – [3d] T. Kruck, F.-J. Becker, H. Breuer, K. Ehlert, W. Rother, *Z. Anorg. Allg. Chem.* **1974**, 107, 95–100. – [3e] E. E. Isaacs, W. A. G. Graham, *Can. J. Chem.* **1975**, 53, 467–473. – [3f] T. Kruck, W. Molls, *Z. Anorg. Allg. Chem.* **1976**, 420, 159–176.
- [4] B. Schiemenz, B. Antelmann, G. Huttner, L. Zsolnai, *Z. Anorg. Allg. Chem.* **1994**, 620, 1760–1767.
- [5] E. Lindner, H. Behrens, S. Birkle, *J. Organomet. Chem.* **1968**, 15, 165–175.
- [6] J. K. Ruff, *Inorg. Chem.* **1967**, 6, 2080–2082.
- [7] J. Weidlein, U. Müller, K. Dehnicke, *Schwingungsspektroskopie* 2nd ed., Georg Thieme Verlag, Stuttgart, New York, **1988**, 114–117.
- [8] F. A. Cotton, C. S. Kraihanzel, *J. Am. Chem. Soc.* **1962**, 84, 4432–4438.
- [9] W.-W. DuMont, H.-J. Kroth, *Z. Naturforsch. B* **1980**, 35, 700–702.
- [10] E. O. Fischer, L. Knauf, *Chem. Ber.* **1969**, 102, 223–229.
- [11] R. F. Bryan, *J. Chem. Soc. A* **1967**, 192–201.
- [12] [12a] R. F. Bryan, P. T. Greene, P. F. Stokely, A. R. Manning, *Chem. Comm.* **1969**, 722–723. – [12b] G. A. Melson, P. F. Stokely, R. F. Bryan, *J. Chem. Soc. A* **1970**, 2247–2251.
- [13] P. T. Greene, R. F. Bryan, *J. Chem. Soc. A* **1970**, 1696–1702.
- [14] U. Müller, N. Mronga, C. Schumacher, K. Dehnicke, *Z. Naturforsch. B* **1982**, 37, 1122–1126.
- [15] T. Szymanska-Buzar, T. Glowiak, *J. Organomet. Chem.* **1995**, 489, 207–214.
- [16] F. Ettel, G. Huttner, L. Zsolnai, C. Emmerich, *J. Organomet. Chem.* **1991**, 414, 71–87.
- [17] A. Tzschach, K. Jurkschat, M. Scheer, J. Meunier-Piret, M. Van Meerse, *J. Organomet. Chem.* **1983**, 259, 165–170.
- [18] [18a] J. D. Cotton, P. J. Davidson, D. E. Goldberg, M. F. Lappert, K. M. Thomas, *Chem. Comm.* **1974**, 893–895. – [18b] J. D. Cotton, P. J. Davidson, M. F. Lappert, *J. Chem. Soc. Dalton Trans.* **1976**, 2275–2286.
- [19] S. L. Ellis, P. B. Hitchcock, S. A. Holmes, M. F. Lappert, M. J. Slade, *J. Organomet. Chem.* **1993**, 444, 95–99.
- [20] B. Wrackmeyer, *Annu. Rev. NMR Spec.* **1985**, 16, 73–186.
- [21] M. F. Lappert, R. S. Rowe, *Coord. Chem. Rev.* **1990**, 100, 267–292.
- [22] R. S. Drago, *Physical Methods in Chemistry*, W. B. Saunders Company, Philadelphia, Eastbourne, Toronto, **1977**.
- [23] D. H. Harris, M. F. Lappert, J. S. Poland, W. McFarlane, *J. Chem. Soc. Dalton Trans.* **1975**, 311–316.
- [24] G. Huttner, *J. Organomet. Chem.* **1986**, 308, C11–C13.
- [25] B. Schiemenz, G. Huttner, L. Zsolnai, P. Kircher, T. Diercks, *Chem. Ber.* **1995**, 128, 187–191.
- [26] A. F. Hollemann, E. Wiberg, N. Wiberg, *Lehrbuch der Anorganischen Chemie* 91th–100th ed., Walter de Gruyter, Berlin, New York, **1985**, 1103–1108.
- [27] M. S. Holt, W. L. Wilson, J. H. Nelson, *Chem. Rev.* **1989**, 89, 11–49.
- [28] J. Kim, Y. Do, Y. S. Sohn, C. B. Knobler, M. F. Hawthorne, *J. Organomet. Chem.* **1991**, 418, C1–C5.
- [29] F. S. Stephens, *J. Chem. Soc. Dalton Trans.* **1975**, 230–232.
- [30] H. Preut, W. Wolfes, H.-J. Haupt, *Z. Anorg. Allg. Chem.* **1975**, 412, 121–128.
- [31] J. E. O'Connor, E. R. Corey, *Inorg. Chem.* **1967**, 6, 968–971.
- [32] [32a] F. P. Boer, J. H. Tsai, J. J. Flynn, *J. Am. Chem. Soc.* **1970**, 92, 6092–6094. – [32b] F. P. Boer, J. J. Flynn, *J. Am. Chem. Soc.* **1971**, 93, 6495–6503.
- [33] J. von Seyerl, B. Sigwarth, G. Huttner, *Chem. Ber.* **1981**, 114, 727–732.
- [34] A. Strube, G. Huttner, L. Zsolnai, *J. Organomet. Chem.* **1990**, 399, 255–266.
- [35] E. W. Abel, I. S. Butler, J. G. Reid, *J. Am. Chem. Soc.* **1963**, 85, 2068–2070.
- [36] P. J. Smith, L. Smith, *Inorg. Chim. Acta. Rev.* **1973**, 7, 11–33.
- [37] N. W. Alecock, R. E. Timms, *J. Chem. Soc. A* **1968**, 1876–1878.
- [38] J. Hilton, E. K. Nunn, S. C. Wallwork, *J. Chem. Soc. Dalton Trans.* **1973**, 173–175.
- [39] B. P. Bir'yukov, Y. T. Struchkov, K. N. Anisimov, N. E. Kolobova, V. V. Skripkin, *Chem. Commun.* **1967**, 750–751.
- [40] F. Ettel, G. Huttner, W. Imhof, *J. Organomet. Chem.* **1990**, 397, 299–307.
- [41] F. Ettel, M. Schollenberger, B. Schiemenz, G. Huttner, L. Zsolnai, *J. Organomet. Chem.* **1994**, 476, 153–162.
- [42] S. J. Davies, N. A. Compton, G. Huttner, L. Zsolnai, S. E. Garner, *Chem. Ber.* **1991**, 124, 2731–2738.
- [43] Promising reactivity is indicated by the observation that **2g** decomposes with a mass loss corresponding to two (OOCCH₃) units at 152°C in a DTG experiment. This observation, however, relates to the solid phase and has not yet been transformed into a preparatively useful reaction, which might be expected on the basis of the potential intermediacy of a $[(\text{CO})_5\text{Cr}]_2\text{Sn}$ species e.g. ref^[44].
- [44] G. K. Magomedov, L. V. Morozova, Y. I. Markova, *Zh. Obshch. Khim.* **1983**, 53, 1684–1685; *J. Gen. Chem. USSR (Engl. Trans.)* **1983**, 53, 1515–1516.
- [45] E. O. Schlemper, *Inorg. Chem.* **1967**, 6, 2012–2017.
- [46] J. A. Zubieta, J. J. Zuckerman, *J. Prog. Inorg. Chem.* **1979**, 24, 251–475.
- [47] [47a] J. T. B. H. Jastrzebski, P. A. van der Schaaf, J. Boersma, G. Van Koten, D. Heijdenrijk, K. Goubiltz, D. J. A. de Ridder, *J. Organomet. Chem.* **1989**, 367, 55–68. – [47b] M. Nardelli, C. Pelizzi, G. Pelizzi, *J. Organomet. Chem.* **1976**, 112, 263–272. – [47c] H.-P. Abicht, K. Jurkschat, A. Tzschach, K. Peters, E.-M. Peters, H. G. von Schnering, *J. Organomet. Chem.* **1987**, 326. – [47d] A. L. Balch, D. E. Oram, *Organometallics* **1988**, 7, 155–158.
- [48] M. D. Brice, F. A. Cotton, *J. Am. Chem. Soc.* **1973**, 95, 4529–4532.
- [49] G. M. Sheldrick, *SHELX86*, Universität Göttingen, **1986**, *SHELX93*, Universität Göttingen, **1993**.
- [50] N. Walker, D. Stuart, *Acta Crystallogr., Sect. A* **1983**, 39, 158–166.

[96005]